Istanbul IABSE Symposium (ISTBR 2023)
April 24 – 26, 2023
Istanbul

1

New challenges in the IABSE TG3.1 benchmark on super long span bridge aerodynamics

Giorgio Diana
Giorgio.diana@polimi.it
Politecnico di Milano, Department of Mechanical Engineering
Milan, Italy

Stoyan Stoyanoff
Stoyan.stoyanoff@rwdi.com
RWDI
Guelph, Canada

……..

and other IABSE TG3.1 members (Andrew Allsop, Luca Amerio, Michael S. Andersen, Tommaso Argentini, Filippo Calamelli, Miguel Cid Montoya, Vincent de Ville, Santiago Hernández, José Ángel Jurado, Igor Kavrakov, Guy Larose, Allan Larsen, Guido Morgenthal, Daniele Rocchi, Roberto Rossi, Martin Svendsen,Teng Wu**)**

ABSTRACT

In the last years, extreme climate events as thunderstorm and downburst are becoming increasingly frequent and widespread. These phenomena could significantly impact on the dynamic response of super long-span bridges since they are typically characterized by a sudden variations of the mean wind speed combined with large vertical angles of attack. This contingency is considered an interesting opportunity for the IABSE Task group 3.1, involved for the last 5 years in the benchmark of the software for the computation of the bridge response to the turbulent wind, to extend the applicability of the consolidated numerical procedures to a case of study characterized by a non-synoptic wind. To reach this purpose, taking as a target the full-scale data measured on the Gjemnessund Bridge during two different incoming wind conditions, a comparison with numerical results is proposed. Specifically, the working group has defined two steps of increasing complexity. The first, given the same input data to the participants, consists of a preliminary numerical benchmark while, the second, concerns the comparison between the outcomes and the dynamic response of the real bridge. In this paper, the results of the wind tunnel tests, performed to measure all the aerodynamic coefficients required for numerically simulating the bridge response, are reported. Finally, the first step is presented and some preliminary outcomes are shown.

Keywords: long-span bridge, full scale monitoring, buffeting response, numerical simulations, wind tunnel tests.

1 INTRODUCTION

In the recent years, extreme climate events characterized by non-synoptic winds are becoming more and more severe and frequent. Phenomena such as thunderstorms and downbursts are typically characterized by sudden variations of the mean wind speed that, combined with large angles of attack could have a significant impact on the dynamic response of long-span bridges. In this context, the IABSE Task Group 3.1 proposal is to investigate the applicability of the numerical methods, typically used to foresee the buffeting response and the aerodynamic stability of long-span bridges due to a synoptic wind, to a non-synoptic case of study. The validation of the numerical approaches by comparison with experimental data is not straightforward, both considering wind tunnel tests and full-scale measurements. Specifically, in this last case, it is not easy to collect all the wind input data and the related output response on a real bridge.

The monitoring campaign carried out from 2018 to 2021 on the Gjemnessund Bridge (Andersen, Isaksen and Ole Hansen, 2021) was identified as a good opportunity to achieve this task as it fulfilled all the relevant requirements. Specifically:

- structural response and wind field data availability. Anemometers, accelerometers and pressure taps were installed on several sections along the bridge, allowing the assessment of the wind field and of the structural response correlation;
- reliable measurements of two wind scenarios: a first case that can be considered synoptic and a second one characterized by a sudden change in mean wind speed combined with a significant variation of the angle of attack;
- bridge sufficiently long and slender to have a relevant dynamic response if invested by a turbulent wind.

Therefore, the Task Group (TG) decided, as final step of the benchmark activity (Diana et al., 2019) (Diana et al., 2020) (Diana et al., 2022) to employ the wind field measurements on the Gjemnessund bridge as common input data for the numerical procedures and to validate the related results with the full-scale response. In particular, this final stage is divided in two phases gradually becoming more and more challenging:

- step 3.1, consists of a numerical versus numerical comparison of the results given the same input data. The purpose is to preliminary benchmark the outcomes of the TG members using simplified cases. This phase is structured in two sub-step:
  - step 3.1a, in which synthetic synoptic wind time histories are considered as input for the numerical simulations;
  - step 3.1b, in which non-synoptic wind time histories are considered as input for the numerical simulations.
- Step 3.2, the results of the TG members will be compared with the full-scale measured response of the case of interest.

The paper is structured as follows. As first, the case of study of the Gjemnessund bridge is briefly presented. Afterwards, wind tunnel tests performed to assess the aerodynamics of the bridge deck are introduced. In Chapter 4, the step 3.1a is presented and the first preliminary results are provided. Finally, some conclusions are drawn and the future steps are introduced.

2 THE CASE OF STUDY: GJEMNESSUND BRIDGE

The monitoring campaign on the Gjemnessund bridge was identified as suitable to achieve the goal of the TG3.1. Specifically, this suspended bridge is characterized by a span length equal to 623 m and a slender steel box girder, shown in Figure 2-1, of dimensions $B \times D$ = 13.2 m × 2.5 m. Moreover, due also to the low natural frequencies (Table 2-1), the bridge is highly sensitive to turbulent winds with a behavior very similar to long-span bridges.

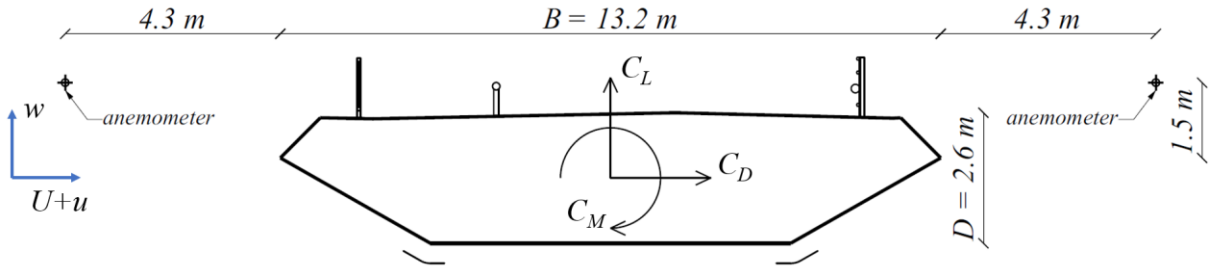

Figure 2-1. Cross section of the Gjemnessund Bridge box girder.

From 2018 to 2021 a monitoring system, composed by anemometers, accelerometers and pressure sensors positioned in several sections along the bridge, was installed on the structure (for details about the monitoring system refers to Andersen, Isaksen and Ole Hansen (2021). Specifically,

at the bridge deck level, a pair of anemometers was installed in five different sections, all arranged on one longitudinal side of the bridge, covering a span-wise distance of approximately six times the deck width. Accelerometers, on the other hand, were installed on several sections along the entire deck.

The full-scale lateral location of the anemometers is shown in Figure 2-1. As it will be described in detail in section 3.2, due the presence of the deck the wind flow at the location of the anemometers is deflected and thus, the measurements of the wind vertical angles of attack was properly corrected.

During the campaign, two events of particular interests were recorded and published in the literature. The first is characterized by a synoptic wind with an average along-wind speed over 10 minutes of approximately 12 m/s and turbulence intensity of 12 %. During the second, on the other hand, a non-synoptic wind was recorded. Specifically, it combines a strong variation of the mean wind speed, approximately from 15 m/s to 25 m/s, with relevant angles of attack. Moreover in this last case, a significant dynamic response of the bridge was registered.

In Figure 2-2 and Figure 2-3 an example of the recorded data is reported for both the events. The data include the correction of the angles of attack as described in section 3.2.

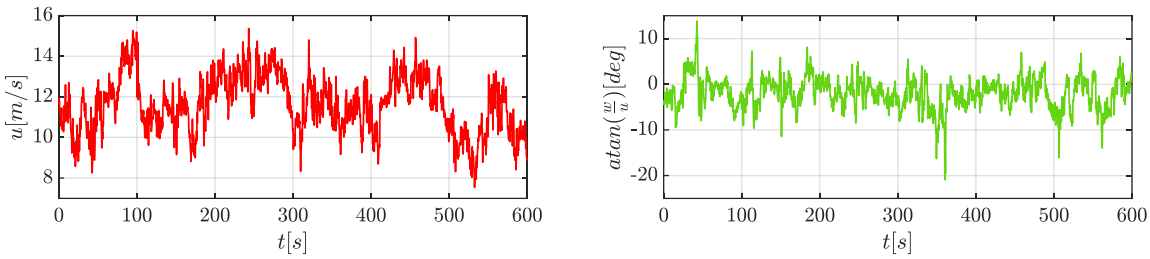

Figure 2-2. Synoptic time histories of the horizontal wind speed and of the vertical angle of attack.

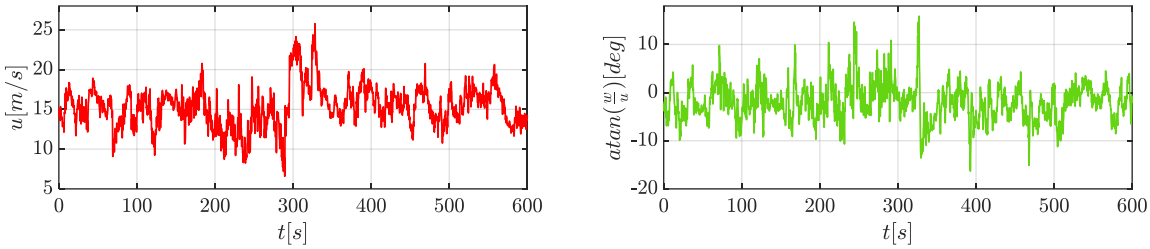

Figure 2-3. Non-synoptic time histories of the horizontal wind speed and of the vertical angle of attack.

2.1 Finite Element model

The 3D structural model of the Gjemnessund Bridge was created based on the available data from literature with the use of the commercial software SAP2000. The modal frequencies, resulting from the finite element model, are consistent with the experimental ones identified from the full-scale measurements. The main modes of the deck are summarized in Table 2-1.

Mode	Frequency [Hz]	Exp. Frequency [Hz]
LS1	0.09	0.09
VA1	0.17	0.17
VS1	0.22	0.22
LA1	0.25	0.26
VS2	0.30	0.30
VA2	0.40	0.39
VS3	0.55	0.53
LS2	0.56	0.54
VA3	0.72	0.70
TS1	0.72	0.78
TA1	1.22	1.31

Table 2-1. Main modal frequencies resulting from the FE model and the corresponding ones identified the from the field measurements.

3 WIND TUNNEL TESTS

The tests were carried out in the Politecnico di Milano wind tunnel. Specifically, the measurement of the aerodynamic properties of the Gjemnessund bridge deck was performed in the low-turbulence test section (turbulence intensity of the flow approximately equal to 0.1%) which is 4m wide, 3.84m high and 6m long and characterized by a maximum wind speed of 55 m/s.

The tests were performed employing the Gjemnessund bridge deck sectional model depicted in Figure 3-1. In particular, the model length scale has been defined as 1:15. According to this scale the outer measure B of the deck chord is equal to 880 mm. The model length L is close to the test section width and is equal to 3980 mm. Therefore, the model aspect ratio L/B is equal to 4.52.

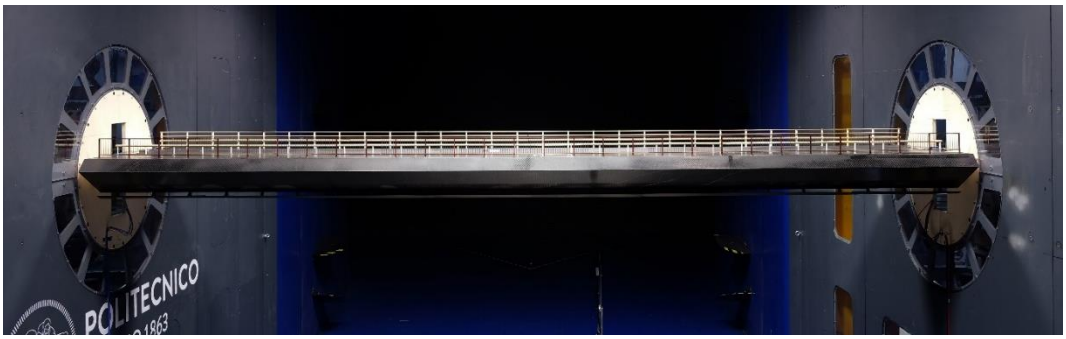

Figure 3-1. Upwind view of the Gjemnessund bridge deck sectional model positioned in the low-turbulence test section of the Politecnico di Milano wind tunnel.

3.1 Correction of the full-scale measured wind angle of attack

As mentioned in the previous sections, the monitoring system of the Gjemnessund bridge is characterized by a series of anemometers positioned at a lateral distance equal to 4.3 m from the windward edge of the deck. At the location of the instrument, the presence of the deck itself deflects the wind flow and thus, the measurement of the angles of attack needs to be adjusted.

At first, the correction to be applied was numerically quantified with 2D RANS Computational Fluid Dynamic simulations. In particular, the deck was statically rotate with respect to the horizontal homogeneous inflow and, for each rotation, the deviation of the wind was measured at the position of the anemometer. To validate the numerical results, the procedure was experimentally repeated in the low-turbulence test section of the Politecnico di Milano wind tunnel. Specifically, a cobra probe was positioned upwind with respect to the sectional model in correspondence of the full-scale anemometer location, as depicted in

Figure 3-2. Afterwards, as performed numerically, the deflection of the flow was measured for different angles of rotation of the deck.

From both procedures, which show good agreement of the results as shown in Figure 3-3, it seems that the absolute value of the wind angle of attack is systematically increased by the presence of the structure. Subsequently, the wind tunnel measurements were employed to correct the initial full-scale wind angle of attack. Figure 3-4 reports, as an example, the correction of the wind angle of attack measured by the anemometer son13 during the non-synoptic event.

Figure 3-2. Cobra probe positioned in correspondence of the full-scale anemometer location.

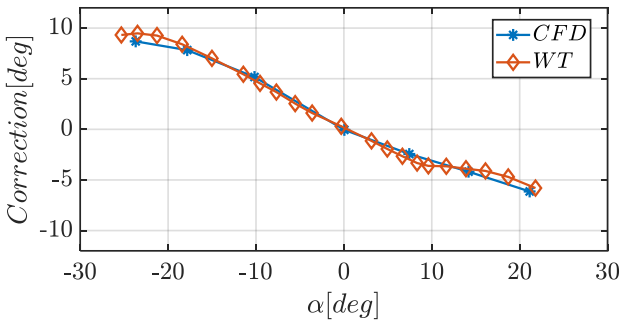

Figure 3-3. Numerical and experimental correction of the angle of attack, reported on the vertical axis, as a function of the measurement of the anemometer, reported on the horizontal axis. Specifically, if the deck rotation is positive (nose-up) the wind angle of attack is increased, with respect to the wind reference system reported in Figure 2-1. On the other hand, if the deck rotation is negative (nose-down), the wind angle of attack is decreased.

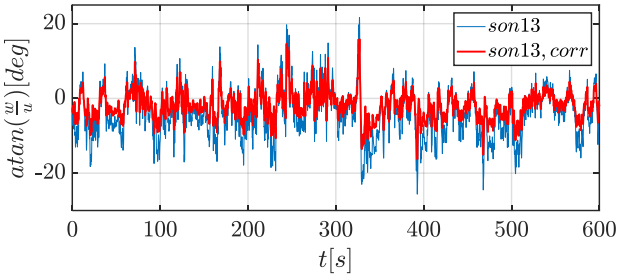

Figure 3-4. Wind angle of attack recorded by the anemometer son13 during the gust and corrected to account for the deflection due to the presence of the deck itself.

3.2 Static aerodynamic coefficients and aerodynamic derivatives

The definition of the static aerodynamic coefficients is mandatory to assess the aerodynamic forces and thus to predict the aeroelastic response of the bridge to turbulent winds. Specifically, the aforementioned coefficients are reported according to the following formulations:

$$C_D = \frac{F_D}{qB} \tag{3-1}$$

$$C_L = \frac{F_L}{qB} \tag{3-2}$$

$$C_M = \frac{M}{qB^2} \tag{3-3}$$

where $q = \frac{1}{2}\rho V^2$ is the mean dynamic wind pressure, with ρ air density and V mean wind speed. F_D, F_L and M are respectively the drag force, the lift force and the pitching moment per unit length. The

reference system employed is reported in Figure 2-1. As already mentioned, the identification of the aerodynamic coefficients was performed for a wide range of wind angles of attack, in particular from -15° to 15°, in order to be able to numerically simulate a non-synoptic wind case with these characteristics. Figure 3-5 depicts the identified static coefficients for the Gjemnessund bridge deck.

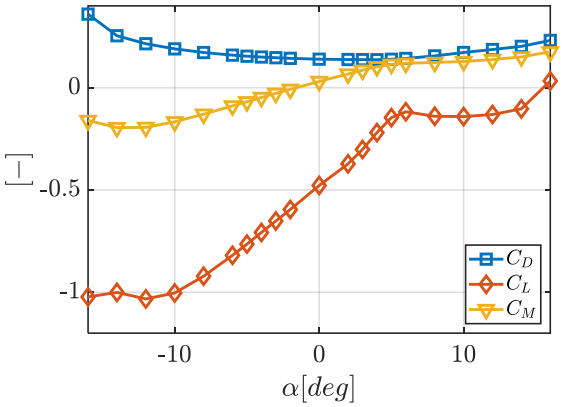

Figure 3-5. Static aerodynamic coefficients of the Gjemnessund bridge deck, defined according to Eq. (3-1), (3-2) and (3-3).

The self-excited forces are here defined employing the aerodynamic derivatives (or flutter derivatives) according to the PoliMi formulation (Zasso, 1996) reported below:

$$D_{se} = \frac{1}{2}\rho V^2 B\left(-p_1^*\frac{\dot{z}}{V} - p_2^*\frac{B\dot{\theta}}{V} + p_3^*\theta + \frac{2\pi^3}{V^{*2}}p_4^*\frac{z}{B} - p_5^*\frac{\dot{y}}{V} + \frac{2\pi^3}{V^{*2}}p_6^*\frac{y}{B}\right) \quad (3\text{-}4)$$

$$L_{se} = \frac{1}{2}\rho V^2 B\left(-h_1^*\frac{\dot{z}}{V} - h_2^*\frac{B\dot{\theta}}{V} + h_3^*\theta + \frac{2\pi^3}{V^{*2}}h_4^*\frac{z}{B} - h_5^*\frac{\dot{y}}{V} + \frac{2\pi^3}{V^{*2}}h_6^*\frac{y}{B}\right) \quad (3\text{-}5)$$

$$M_{se} = \frac{1}{2}\rho V^2 B^2\left(-a_1^*\frac{\dot{z}}{V} - a_2^*\frac{B\dot{\theta}}{V} + a_3^*\theta + \frac{2\pi^3}{V^{*2}}a_4^*\frac{z}{B} - a_5^*\frac{\dot{y}}{V} + \frac{2\pi^3}{V^{*2}}a_6^*\frac{y}{B}\right) \quad (3\text{-}6)$$

with p_{1-6}^*, h_{1-6}^* and a_{1-6}^* aerodynamic derivatives, y, z and θ respectively lateral, vertical and torsional motion of the bridge deck and $V^* = \frac{V}{fB}$ reduced velocity, where f is the frequency employed for the forced motion tests. The forcing of the model was performed with a test-rig with electrodynamic controlled actuators. Furthermore, this setup allows for the measurements of the aerodynamic forces related to the torsional, vertical, and horizontal motion of the deck, employing two 6-axis balances positioned at the deck extremities. The aerodynamic derivatives were identified for 20 combinations of mean wind speed and frequency of the imposed harmonic motion, for a range of reduced velocities between 1.1 and 45.5. Table 3-1 resumes the parameters employed for the tests. The amplitude of the torsional harmonic motion was set equal to 1° while, for the vertical forcing, it was set to have an equivalent torsional rotation of 1°. Moreover, the identification was performed around a range of static angles between -6° and 6°. The reason is that the time history of the "corrected" wind angle of attack, recorded during the gust and low-pass filtered with a cut frequency of 0.05 Hz, is approximately included between the aforementioned range, see. Figure 3-6. A selection of aerodynamic derivatives is reported in Figure 3-7.

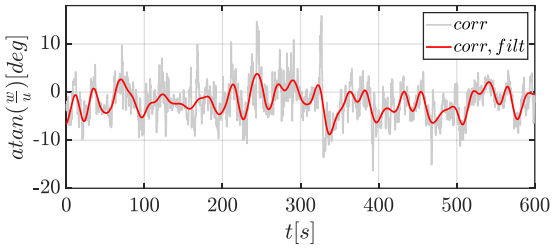

Figure 3-6. Time history of the angle of attack related to the non-synoptic wind. Both curve are corrected as reported in Section 3.1, the red one is also low-pass filtered with a cut-off frequency of 0.05 Hz.

Static angles [deg]	Mean wind speeds [m/s]	Frequencies [Hz]
0, ±3, +5, ±6	5, 10, 15, 20	0.5, 1, 2, 4, 5

Table 3-1. Parameters employed for the identification of the aerodynamic derivatives.

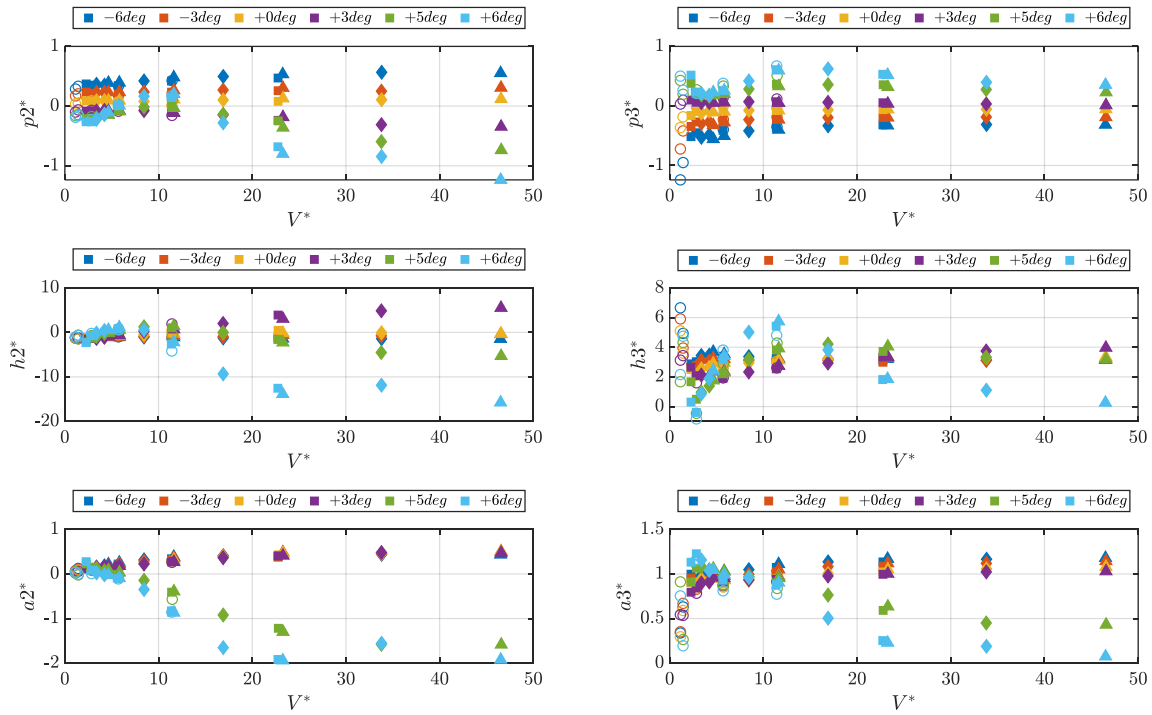

Figure 3-7. Aerodynamic derivatives identified forcing the Gjemnessund bridge deck sectional model with an harmonic torsional motion. Different markers are employed for different experimental mean wind speed. Specifically: ○= 5 m/s, ■ = 10 m/s, ♦ = 15 m/s and ▲= 20 m/s. It is worth noting that the flutter derivatives measured with $V = 5$ m/s are not completely reliable since the aerodynamic forces are too low to be correctly measured by the dynamometric balances.

4 BENCHMARK: STEP 3.1a

As already mentioned, the first step of the activity consists in a numerical comparison of the results of the TG members, given the same input data. In particular, the sub-step 3.1a is a preliminary simplified phase to benchmark the outcomes of the different numerical procedures considering the case of study of the Gjemnessund bridge. The input data are defined as follows:

- incoming turbulent wind: an harmonic superposition method is employed for the generation of the synoptic wind time histories. The parameters used are briefly reported in Table 4-1;
- structural data: the characteristics of the numerical model of the Gjemnessund bridge are reported in Section 2.1;

- aerodynamics: the aerodynamic forces of the Gjemnessund bridge deck are experimentally identified with wind tunnel tests and reported in Section 3.2.

Wind speeds	$U = 12, 24, 36\ m/s$
Air density	$\rho = 1.22\ kg/m^3$
Turbulence intensity	$I_u = \frac{\sigma_u}{U} = 0.12;\ I_w = \frac{\sigma_w}{U} = 0.05$
Integral length scale	${}^xL_u = 175\ m;\ {}^xL_w = 50\ m$

Table 4-1. Parameters used for the generation of the synoptic wind time histories.

As a preliminary result, Figure 4-1. Total damping ratio as a function of the mean wind speed.Figure 4-1 shows the total damping ratio of the unstable mode as a function of the mean wind speed, highlighting a flutter critical wind speed approximately equal to 105.5 m/s. Furthermore, the numerical time histories of the lateral, vertical and torsional midspan displacements are depicted in Figure 4-2. The results refer to the wind scenario characterized by a mean wind speed equal to 36 m/s. The curves depicted are in a quite good agreement, with some differences in the torsional displacement.

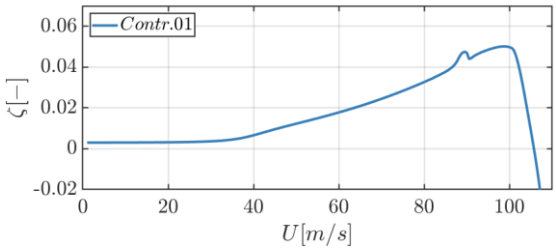

Figure 4-1. Total damping ratio as a function of the mean wind speed.

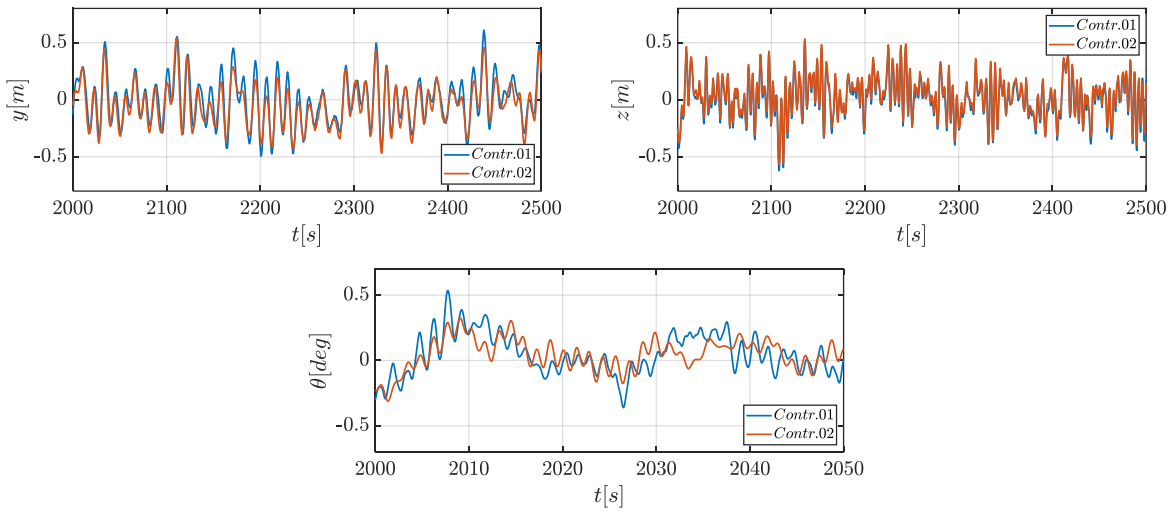

Figure 4-2. Two contribution for the detrended lateral, vertical and torsional midspan displacements related to the wind time histories characterized by a mean wind speed equal to 36 m/s.

5 CONCLUSIONS AND FUTURE DEVELOPMENTS

A comparison between numerical simulation and full-scale measurements on a real bridge is proposed by the IABSE TG3.1. Specifically, the main goal of the working group is to extend the validation of consolidated numerical methods to a non-synoptic wind case of study. The Gjemnessund bridge monitoring campaign was identified as a good opportunity to reach this purpose. In this paper, the first sub-step of the benchmark activity is presented and the wind tunnel tests, performed to

identify all the required aerodynamic coefficients, are described. Finally, some preliminary results are provided.

The future steps will be focused on the numerical application of non-synoptic winds and on the comparison with the measurements on the real bridge. In this last step, a particular difficulty will be presented by the application of the wind time histories, measured in specific sections of Gjemnessund bridge, to all the other longitudinal position present in the numerical model.

REFERENCES

[1] M. Andersen, B. Isaksen and S. Ole Hansen, 2021. “Full-Scale Monitoring of the Wind Field, Surface Pressures and Structural Response of Gjemnessund Suspension Bridge”, Struct. Eng. Int.

[2] G. Diana, S. Stoyanoff, K. Aas-Jakobsen, A. Allsop, M. Andersen, T. Argentini, M. Cid Montoya, S. Hernández, J. Á. Jurado, H. Katsuchi, I. Kavrakov, H. Kim, G. Larose, A. Larsen, G. Morgenthal, O. Øiseth, S. Omarini, D. Rocchi, M. Svendsen and T. Wu, 2019. "IABSE Task Group 3.1 Benchmark Results. Part 1: Numerical Analysis of a Two-Degree-of-Freedom Bridge Deck Section Based on Analytical Aerodynamics", Struct. Eng. Int., vol. 30, pp. 401-410.

[3] G. Diana, S. Stoyanoff, K. Aas-Jakobsen, A. Allsop, M. Andersen, T. Argentini, M. Cid Montoya, S. Hernández, J. Á. Jurado, H. Katsuchi, I. Kavrakov, H. Kim, G. Larose, A. Larsen, G. Morgenthal, O. Øiseth, S. Omarini, D. Rocchi, M. Svendsen and T. Wu, 2020. "IABSE Task Group 3.1 Benchmark Results. Part 2: Numerical Analysis of a Three-Degree-of-Freedom Bridge Deck Section Based on Experimental Aerodynamics", Struct. Eng. Int., vol. 30, pp. 411-420.

[4] G. Diana, S. Stoyanoff, K. Aas-Jakobsen, A. Allsop, L.Amerio, M. Andersen, T. Argentini, F. Calamelli, M. Cid Montoya, V. de Ville de Goyet, S. Hernández, J. Á. Jurado, I. Kavrakov, G. Larose, A. Larsen, G. Morgenthal, D. Rocchi, M. Svendsen and T. Wu, 2022. "IABSE Task Group 3.1 Benchmark Results. Numerical Full Bridge Stability and Buffeting Simulations", Struct. Eng. Int.

[5] A. Zasso, 1996. "Flutter derivatives: Advantages of a new representation convention", J. Wind Eng. Ind. Aerodyn., vol. 60, pp. 35-47.

A more extensive and adequate bibliography can be found in [2] [3] and [4].